ELSEVIER

Thermochimica Acta 372 (2001) 165–173

thermochimica acta

www.elsevier.com/locate/tca

Organic–inorganic hybrid materials Part 9: Dynamics and stability of PMMA modified aluminum–EAA complex

T.C. Chang[a,*], Y.T. Wang[a], Y.S. Hong[a], Y.S. Chiu[b]

[a]*Department of Applied Chemistry, Chung Cheng Institute of Technology, NDU Tahsi, Taoyuan 335, Taiwan, ROC*
[b]*Chemical Systems Research Division, Chung Shan Institute of Science and Technology, Taoyuan 325, Taiwan, ROC*

Received 24 November 2000; accepted 11 January 2001

Abstract

Poly(methyl methacrylate) (PMMA) containing aluminum–ethyl acetoacetate (EAA) [M5-Al(OBu^s)(EAA)$_2$] was obtained from trialkoxysilane-functional poly(methyl methacrylate) and ethyl acetoacetate modified aluminum sec-butoxide via the sol–gel method. Infrared (IR), ^{13}C nuclear magnetic resonance (NMR) spectroscopy, and thermogravimetric analysis (TGA) were used to analyze the structures and properties of the hybrids with various proportions of PMMA. The effects of the PMMA content on the dynamics and stability of the M5-Al(OBu^s)(EAA)$_2$ hybrids were investigated in this study. The ^{1}H spin-diffusion path length of the hybrids was in a nanometer scale as estimated from the spin–lattice relaxation time in a rotating frame ($T_{1\rho}^{H}$). The apparent activation energies (E_a), evaluated by van Krevelen's method, of the M5-Al(OBu^s)(EAA)$_2$ in thermo-oxidative degradation for random scission of EAA segments decreased roughly with increasing PMMA content.

Keywords: Poly(methyl methacrylate); Aluminum alkoxide; Hybrids; Relaxation; Degradation

1. Introduction

At present, popular ceramic substrates used in the industry are made of alumina or its composites because of their excellent thermal and mechanical properties. Organic polymers combined with inorganic components, especially metal alkoxides, chemically modified with chelating ligands, have been synthesized by the sol−gel process in order to prevent the precipitation during hydrolysis and condensation. Ethyl acetoacetate (EAA) is generally used to stabilize aluminum alkoxides [1–4].

Several methods have been used to characterize the miscibility of organic–inorganic hybrids, including microscopy, scattering techniques, mechanical and thermal measurements, and spectroscopy. NMR spectroscopic methods are sensitive to short range interactions. The relaxation processes can be influenced by several factors, such as change in molecular mass and addition of a suitable polymer modifier. In our previous work, the miscibility of poly(methyl methacrylate)–silica (PMMA–SiO_2) and polyvinylimidazole–silica (PVI–SiO_2) hybrids was studied by NMR

* Corresponding author. Tel.: +886-3-389-1716; fax: +886-3-389-2711.
E-mail address: techuan@ccit.edu.tw (T.C. Chang).

0040-6031/01/$ – see front matter
PII: S0040-6031(01)00447-6

with relaxation time measurement, and it was found that the organic and inorganic segments separated on a nanometer scale as estimated by spin-diffusion path length [5,6]. On the other hand, investigations of thermal decomposition parameters, such as E_a, ΔH^*, ΔS^*, and ΔG^* have been carried out on the transition metal complexes of various classes of organic ligands [7–11]. But, very little work has been carried out on the dynamic and thermal stability of poly(methyl methacrylate) modified by ceramic precursor such as $Al(OBu^s)(EAA)_2$, i.e. aluminum sec-butoxide complex with ethyl acetoacetate.

In the present study, poly(methyl methacrylate) containing aluminum–ethyl acetoacetate hybrid materials, M5-$Al(OBu^s)(EAA)_2$, were prepared by the sol–gel technique. To understand the dynamics of the hybrids, the proton spin–lattice relaxation times in the rotating frame ($T_{1\rho}^{H}$) of the hybrids were measured. Furthermore, the thermo-oxidative stability of the $Al(OBu^s)(EAA)_2$ complex containing various proportions of PMMA was measured by thermogravimetric analysis. The values of apparent activation energy (E_a) were evaluated by van Krevelen's method [12].

2. Experimental

2.1. Materials

The monomer methyl methacrylate (MMA, Janssen) was purified by distillation before use, [3-(methacryloxy)propyl]trimethoxysilane (MSMA, TCI) was used without purification. Aluminum sec-butoxide [$Al(OBu^s)_3$, Strem] was used as the inorganic source and it is commercially available. Ethyl acetoacetate (EAA, Janssen) was used as a chemical modifier of aluminum alkoxide in order to prevent the precipitation on the hydrolysis of aluminum alkoxide. Azobis(isobutyronitrile) (AIBN, BDH) was recrystallized from ethanol prior to use. Tetrahydrofuran (THF, Aldrich) was fractionally distilled in the presence of metallic sodium and benzophenone under nitrogen atmosphere. Deionized water (18 MΩ) was used for the hydrolysis.

2.2. Preparation of M5-$Al(OBu^s)(EAA)_2$ hybrids

PMMA containing aluminum–EAA hybrids, M5-$Al(OBu^s)(EAA)_2$, were prepared in situ by sequential

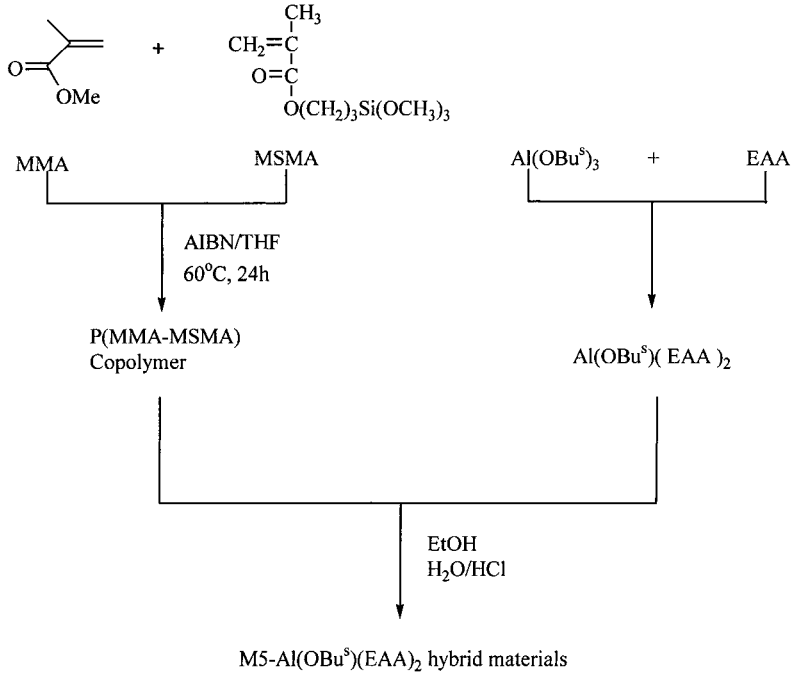

Scheme 1.

synthesis, as outlined in Scheme 1. In a typical example, a mixture of MMA (4.00 g) and MSMA (0.524 g), AIBN (6.89×10^{-3} g), and THF (28 ml) was poured into a 100 cm^3 round bottom flask under nitrogen, and the solution stirred for 24 h at 60°C to initiate the copolymerization of the methacrylic monomers. A homogeneous solution of $Al(OBu^s)_3$ (6.786 g) and EAA (7.170 g) was added, followed by addition of water (0.992 g) and ethanol (5.068 g). After stirring for 30 min at room temperature, the mixture was allowed to gel at room temperature for a week. The hybrid was further heated for 24 h at 70°C, 3 h at 100°C, and finally 24 h at 150°C under vacuum. Hybrid M5-$Al(OBu^s)(EAA)_2$-60 was obtained, where 60 denotes that 60 wt.% of $Al(OBu^s)_3$ based on weight of monomer (MMA and MSMA) and $Al(OBu^s)_3$ condenses with 40 wt.% of PMMA with 5 mol% trialkoxysilyl functional group. The formulations of the other hybrids are listed in Table 1.

2.3. Characterization of M5-$Al(OBu^s)(EAA)_2$ hybrids

The IR spectrum of the samples dispersed in dry KBr pellets were recorded between 4000 and 500 cm^{-1}. The ^{13}C, ^{27}Al and ^{29}Si NMR spectra of the solid state M5-$Al(OBu^s)(EAA)_2$ hybrids were measured using a Bruker MSL-400 with the cross-polarization combined with magic angle spinning (CP/MAS). The proton spin−lattice relaxation times in the rotating frame ($T_{1\rho}^{H}$) were measured by using a ^1H spin-lock τ-pulse sequence followed by cross-polarization. The ^1H 90° pulse width was 4.5 μs, and the CP contact time was 2 ms. The length of delay time, τ ranged from 0.1 to 20 ms for $T_{1\rho}^{H}$. The thermal stability of hybrid was measured using a Perkin-Elmer TGA-2 at heating rate of 10°C/min in air. The sample weight was about 10 mg, and the gas flow rate was kept at 100 cm^3/min.

3. Results and discussion

3.1. Hybrids characterization

The IR spectra of M5-$Al(OBu^s)(EAA)_2$ hybrids containing various proportions of PMMA are shown in Fig. 1. The intensities of the peaks, the characteristic of PMMA at 1724 and 750 cm^{-1} (Fig. 1) decrease with decreasing PMMA content, whereas those at 1733, 1604 and 1516 cm^{-1} increased. Absorption peak at 1604 and 1516 cm^{-1}, respectively corresponds to C–O and C=C stretching vibration in the enol form of EAA bonded to $Al(OBu^s)_3$ [13]. The results indicate that the EAA is complexed to $Al(OBu^s)_3$ in the enol form. On the other hand, the band at 1733 cm^{-1} corresponds to a partially released EAA ligand.

The NMR chemical shift is affected by reaction, conformational changes, hydrogen bonding and intermolecular forces, while its shape reflects the mobility of certain parts of the molecules. The ^{27}Al CP/MAS NMR spectra of M5-$Al(OBu^s)(EAA)_2$ hybrids are nearly identical, as shown in Fig. 2. ^{27}Al resonance was broad and asymmetric indicative of the distribution in quardrupolar coupling constants and chemical shift. All the spectra showed an intense resonance at around −1 ppm from octahedral aluminum (Al^{VI}). The resonance at 66 and 35 ppm was assigned to aluminum in four- (Al^{IV}) and five-fold (Al^{V}) coordination, respectively [14]. The results suggest that for PMMA modified $Al(OBu^s)(EAA)_2$ complex treated at temperature below 200°C, generally only octahedral

Table 1
Experimental conditions for M5-$Al(OBu^s)(EAA)_2$ hybrids[a]

Hybrids	P(MMA–MSMA) (wt.%)	$Al(OBu^s)(EAA)_2$ (wt.%)
A: M5-$Al(OBu^s)(EAA)_2$-85	15	85
B: M5-$Al(OBu^s)(EAA)_2$-80	20	80
C: M5-$Al(OBu^s)(EAA)_2$-75	25	75
D: M5-$Al(OBu^s)(EAA)_2$-70	30	70
E: M5-$Al(OBu^s)(EAA)_2$-60	40	60
F: M5-$Al(OBu^s)(EAA)_2$-30	70	30

[a] [MSMA]/([MSMA]+[MMA]) = 0.05; MMA: methyl methacrylate; MSMA: [3-(methacryloxy)propyl]trimethoxysilane; $Al(OBu^s)_3$: aluminum sec-butoxide; EAA: ethyl acetoacetate; $Al(OBu^s)_3$/EAA molar ratio = 1:2.

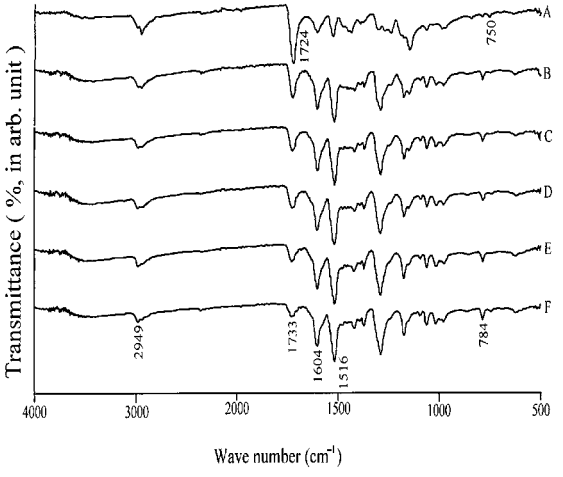

Fig. 1. Infrared spectra of the hybrids: (A) M5-Al(OBu^s)(EAA)$_2$-30; (B) M5-Al(OBu^s)(EAA)$_2$-60; (C) M5-Al(OBu^s)(EAA)$_2$-70; (D) M5-Al(OBu^s)(EAA)$_2$-75; (E) M5-Al(OBu^s)(EAA)$_2$-80; (F) M5-Al(OBu^s)(EAA)$_2$-85.

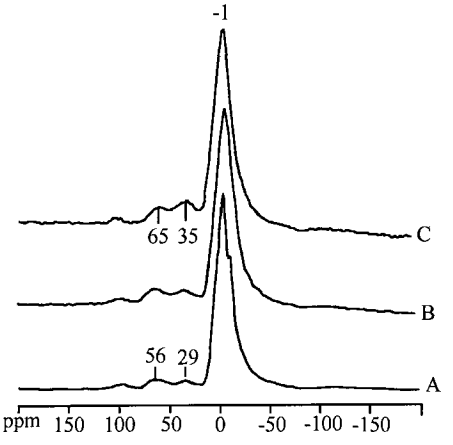

Fig. 2. ^{27}Al CP/MAS NMR spectra of the hybrids: (A) M5-Al(OBu^s)(EAA)$_2$-30; (B) M5-Al(OBu^s)(EAA)$_2$-60; (C) M5-Al(OBu^s)(EAA)$_2$-85.

Al within M5-Al(OBu^s)(EAA)$_2$ hybrids was observed. Note that the resonance of Al^{IV} and Al^{V} in M5-Al(OBu^s)(EAA)$_2$-30 (Fig. 2C) are observed at 56 and 29 ppm. The up field resonance suggests that trialkoxysilane-functional PMMA bonds with aluminum as PMMA bonds are major one in hybrid [15]. ^{29}Si CP/MAS NMR spectrum of M5-Al(OBu$^{s)(EAA)}$$_2$-30 shows a broad peak in the range −40 to −70 ppm (Fig. 3) indicates of most being T^2-species (−56 ppm). Moreover, a faster energy exchanged between the ^{1}H and ^{29}Si spin systems of the T^2-species than that of T^3-species (−65 ppm) is a result of the former contain more protons which can provide the Si–H dipolar coupling, as suggested by previous literature [5], and the relaxation behavior of the T^2-species in M5-Al(OBu^s)(EAA)$_2$-30 hybrid has not much difference with that in PMMA–SiO$_2$ hybrids [5].

Fig. 4 shows the ^{13}C CP/MAS NMR spectrum of M5-Al(OBu^s)(EAA)$_2$-85 hybrid. The chemical shifts for the PMMA segments observed at 178, 56, 52, 45

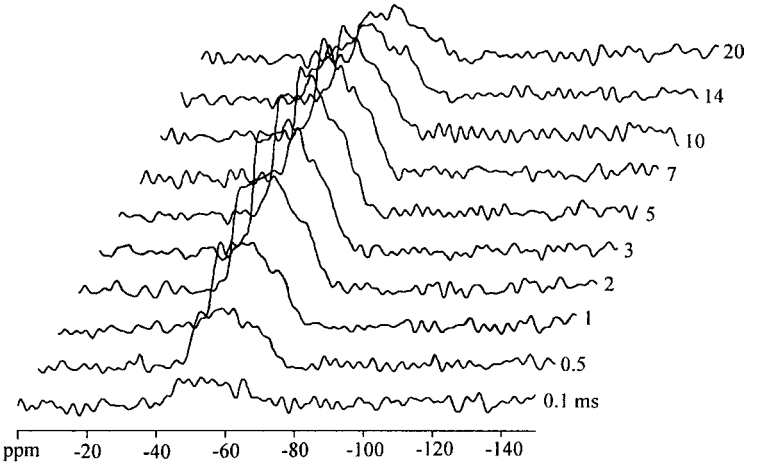

Fig. 3. ^{29}Si CP/MAS NMR spectra of M5-Al(OBu^s)(EAA)$_2$-30 hybrid as a function of contact time.

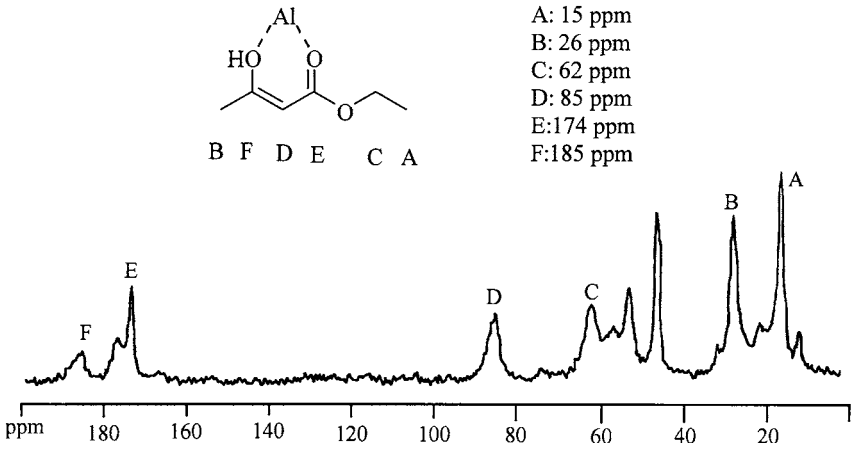

Fig. 4. ^{13}C CP/MAS NMR spectrum of M5-Al(OBu^s)(EAA)$_2$-85 hybrid.

and 18 ppm correspond with the carboxyl, methylene, methoxy, quaternary and methyl carbons, respectively [5,16]. Therefore, the chemical shifts at 185, 174, 85, 62, 26 and 15 ppm are due to the EAA ligand carbons. The resonance at 185 and 174 ppm is attributed to carbonyl carbons in enol form of EAA chelating to aluminum, while those at 85, 62, 26 and 15 ppm are correspond to =C̲H–, –OC̲H$_2$CH$_3$, –CC̲H$_3$, and OCH$_2$C̲H$_3$, respectively [5,16]. On the other hand, the intensity of the methoxy carbon peak (52 ppm) relative to that methylene carbon peak (56 ppm) is independent of the PMMA content in hybrids, and that is similar to the spectrum of bulk PMMA. This suggests no Lewis acid–base interaction between PMMA and Al(OBu^s)(EAA)$_2$ complex [17].

3.2. Hybrids relaxation time

Based on the spin-locking mode employed in $T^{\mathrm{H}}_{1\rho}$ measurement, the magnetization of resonance is expected to decay according to the following exponential function [18]:

$$M_\tau = M_0 \exp\left[\frac{-\tau}{T^{\mathrm{H}}_{1\rho}}\right] \quad (1)$$

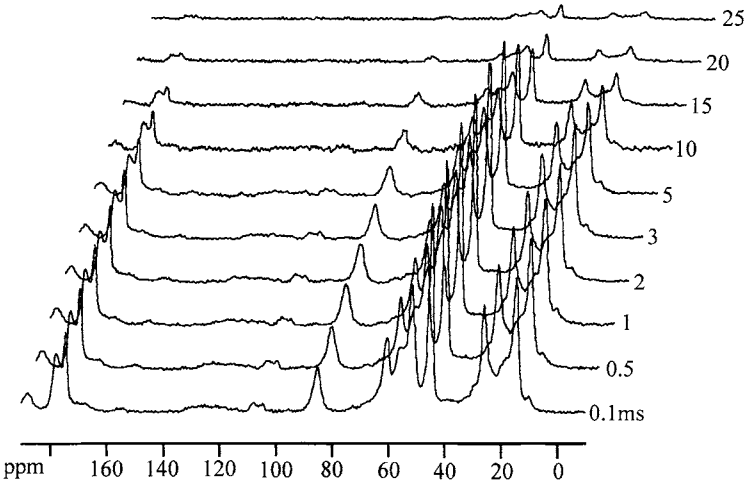

Fig. 5. Stacked plot of the ^{13}C CP/MAS NMR spectra of M5-Al(OBu^s)(EAA)$_2$-60 hybrid as a function of delay time.

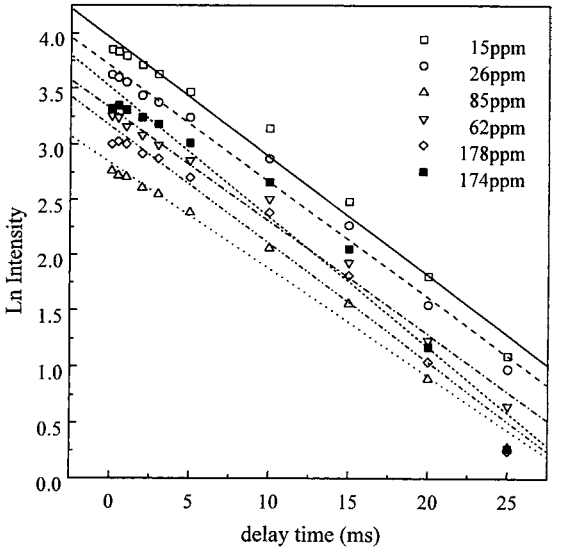

Fig. 6. Semilogarithmic plot of the peak intensity of the M5-Al(OBu^s)(EAA)$_2$-60 hybrid as a function of the delay time.

Here τ is the delay time used in the experiment and M_τ corresponds to resonance intensity. Fig. 5 shows the effect of delay time, τ on the ^{13}C resonance of the M5-Al(OBu^s)(EAA)$_2$-60 hybrid. All the peaks present the same relaxation behavior, indicating no bias due to local environment. The $T_{1\rho}^{H}$ values of the respective carbon in this hybrid can be measured by using the standard pulse sequence, as shown in Fig. 6. Table 2 shows that the $T_{1\rho}^{H}$ value of the PMMA segments (178 ppm) is consistent with that of the EAA segments indicating that they have the same mobility. Moreover, the PMMA content does not affect the relaxation measurement, suggesting that aluminum is intimate with the EAA to the same extent. However, the $T_{1\rho}^{H}$ values of M5-Al(OBu^s)(EAA)$_2$-30 show a larger value as compared with that of the other hybrids (Table 2). This may be due to the fact that the motion of the EAA and PMMA segments in the former is less restricted and becomes looser. Consequently, the spin-diffusion path length (L) of the M5-Al(OBu^s)(EAA)$_2$-30 would be enhance.

A fast spin-diffusion occurs among all the protons in the hybrids, which averages out the whole relaxation process. Thus, the domain size of hybrids is smaller than the spin-diffusion path length within $T_{1\rho}^{H}$ time. The spin-diffusion path length can be estimated using the following equation [18]:

$$\langle L^2 \rangle = \left(\frac{T_{1\rho}^{H}}{T_2} \right) \langle L_0^2 \rangle \quad (2)$$

Here L_0 is the distance between protons, typically 0.1 nm, and T_2 is the spin–spin relaxation time which, below T_g, is about 10 μs, and then, the mean square distance $\langle L^2 \rangle$ over which magnetization can be evaluated. The calculated spin-diffusion path length L is in the range of 3–4 nm (Table 2). This result, therefore, implies that the PMMA segments and Al(OBu$^{s)(EAA)}$$_2$ complex in hybrids are compatible in a scale of several nanometer.

3.3. Thermal stability

Fig. 7 shows the TGA and DTG curves of the M5-Al(OBu^s)(EAA)$_2$ hybrids under air at a heating rate of 10°C/min. M5-Al(OBu^s)(EAA)$_2$ hybrids degrade mainly by a three-stage process, and that is destroyed virtually complete at 600°C. The maximum rate of weight loss at the first stage decreases with increasing

Table 2
The proton spin–lattice relaxation times in the rotating frame $T_{1\rho}^{H}$ values of the respective resonance lines (ppm) of M5-Al(OBu^s)(EAA)$_2$ hybrids, and the spin-diffusion path length L values of hybrids

Hybrids	$T_{1\rho}^{H}$ (ms)							L (nm)
	15	26	62	85	174	178	Average	
A: M5-Al(OBu^s)(EAA)$_2$-85	11.08	10.19	14.52	16.76	15.87	13.46	13.65	3.69
B: M5-Al(OBu^s)(EAA)$_2$-80	8.34	8.68	10.39	10.94	10.05	12.59	10.17	3.19
C: M5-Al(OBu^s)(EAA)$_2$-75	10.24	10.47	10.53	12.90	11.30	13.29	11.46	3.38
D: M5-Al(OBu^s)(EAA)$_2$-70	8.63	9.01	9.25	11.23	11.32	12.04	10.25	3.20
E: M5-Al(OBu^s)(EAA)$_2$-60	9.34	9.59	9.82	10.41	8.56	9.41	9.52	3.09
F: M5-Al(OBu^s)(EAA)$_2$-30	16.40	–	–	–	–	15.80	16.10	4.01

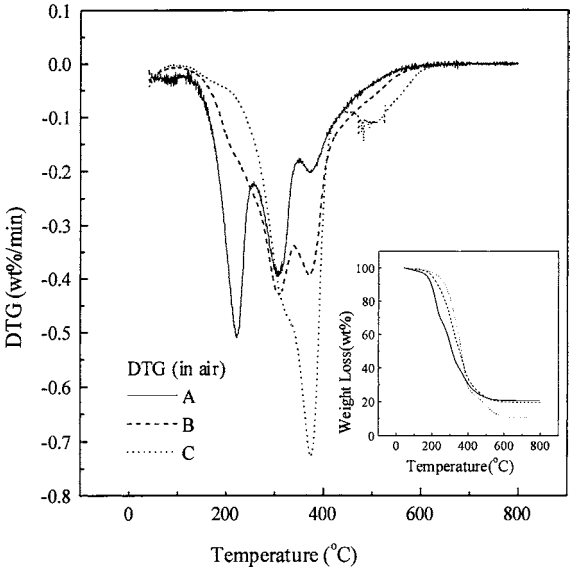

Fig. 7. TGA and DTG thermograms (10°C/min) of hybrid materials under air: (A) M5-Al(OBu^s)(EAA)$_2$-30; (B) M5-Al(OBu^s)(EAA)$_2$-60; (C) M5-Al(OBu^s)(EAA)$_2$-85.

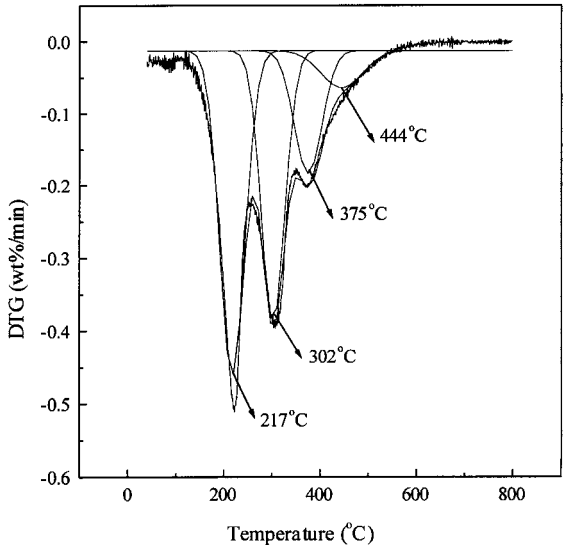

Fig. 8. The deconvoluted DTG curve of M5-Al(OBu^s)(EAA)$_2$-85 hybrid under air.

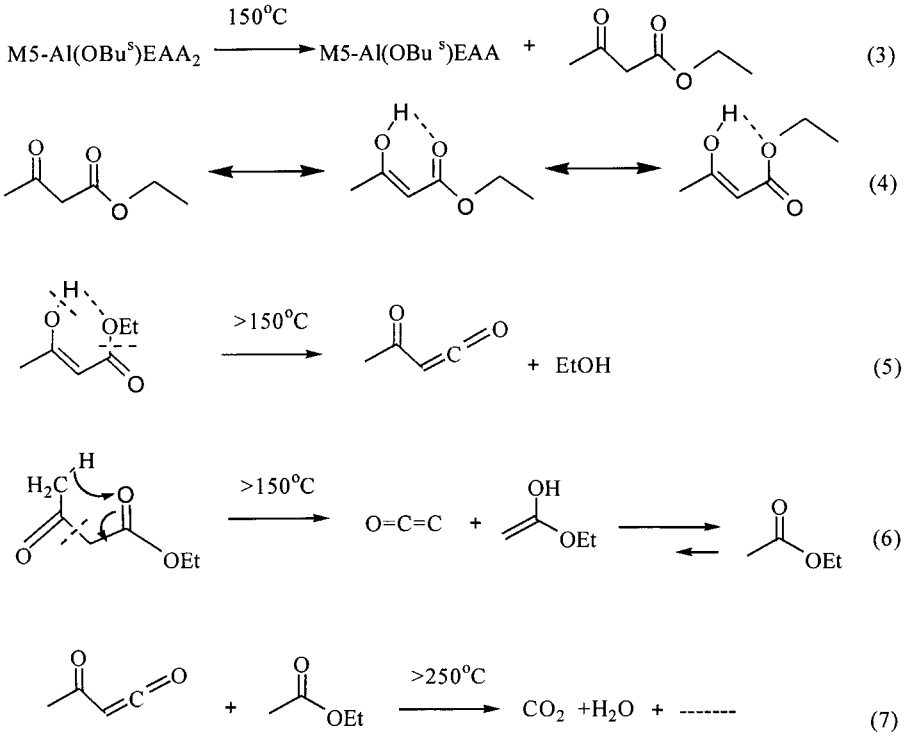

Scheme 2.

Table 3
The characteristic parameters of thermo-oxidative degradation (10°C/min) for hybrid materials[a]

Hybrids	T_{p1} (°C)	T_{p2} (°C)	T_{p3} (°C)	T_{p4} (°C)	n	E_a (kJ/mol)
A: M5-Al(OBu^s)(EAA)$_2$-85	217	302	375	444	1.26	56
B: M5-Al(OBu^s)(EAA)$_2$-80	212	293	375	431	1.26	58
C: M5-Al(OBu^s)(EAA)$_2$-75	215	293	369	419	1.26	41
D: M5-Al(OBu^s)(EAA)$_2$-70	217	304	370	404	1.26	36
E: M5-Al(OBu^s)(EAA)$_2$-60	248	311	371	422	1.26	38
F: M5-Al(OBu^s)(EAA)$_2$-30	231	333	375	494	1.26	34

[a] T_{p1}–T_{p4} are the temperatures of maximum rate of weight loss at the first to fourth stage in fitting curve; n is reaction order in the first stage; E_a is activation energy of degradation in the first stage.

the PMMA content, while that at third stage increases. Therefore, the former weight loss corresponds to Al(OBu^s)(EAA)$_2$ complex and the latter corresponds to PMMA. The deconvoluted DTG curve of M5-Al(OBu^s)(EAA)$_2$-85 hybrid under air shows clearly four-stage (Fig. 8). It can be seen that the peak temperatures (T_p) of each degradation is about 217, 302, 375, and 444°C, respectively. The degradations of the hybrids are consistent with Scheme 2 [19]. The weight loss in the first-stage (~100–250°C) corresponded with step (3)–(6). On the other hand, the last step (>450°C) may be due to the dehydroxylation of Al–OH groups. Moreover, the data of T_p in other hybrids are listed in Table 3. It can be seen that the T_{p1}, T_{p2}, T_{p3}, and T_{p4} are around 220, 300, 370 and 430°C, respectively. The result suggests that the degradation of the hybrids is independent of the PMMA content. Moreover, the T_{p4} value of the M5-Al(OBu^s)(EAA)$_2$-30 is comparatively higher than the other hybrids. This may be rationalized on the basis of the formation of the silica [5,16].

The reaction order (n) of the thermo-oxidative degradation in the first stage, determined by the Kissinger's equation [20], is independent of the PMMA content and that is about 1.26. Fig. 9 shows the logarithmic plot for degradation rate $g(\alpha)$ of the hybrids versus temperature of the first stage. The apparent activation energy E_a of the degradation, evaluated from van Krevelen method [12], is listed in Table 3. We found that the E_a values of random scission for the EAA segments were in the range of 58–34 kJ/mol, and that decreased roughly with increasing the PMMA content. The reduction in E_a revealed that the bonding strength between aluminum and EAA ligand was reduced as the PMMA content increased.

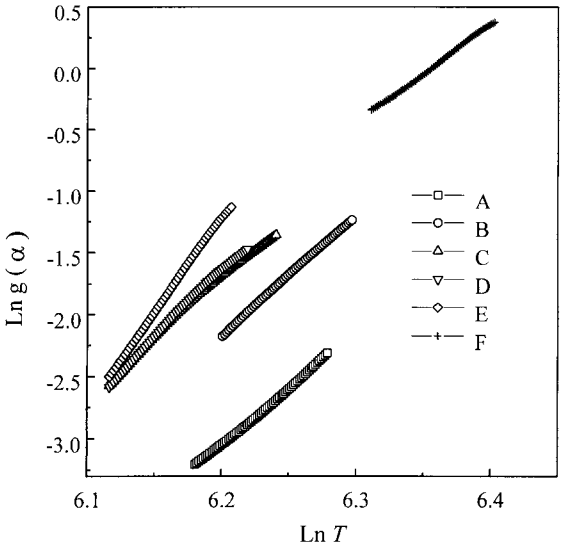

Fig. 9. Plot of ln $g(\alpha)$ vs. ln T for thermo-oxidative degradation (10°C/min) of the hybrids: (A) M5-Al(OBu^s)(EAA)$_2$-30; (B) M5-Al(OBu^s)(EAA)$_2$-60; (C) M5-Al(OBu^s)(EAA)$_2$-70; (D) M5-Al(OBu^s)(EAA)$_2$-75; (E) M5-Al(OBu^s)(EAA)$_2$-80; (F) M5-Al(OBu^s)(EAA)$_2$-85.

4. Conclusions

The M5-Al(OBu^s)(EAA)$_2$ hybrids were prepared via sol–gel techniques by mixing P(MMA–MSMA) copolymer, and aluminum sec-butoxide modified with ethyl acetoacetate. The characterization of the hybrids was confirmed through IR, ^{13}C, ^{27}Al, ^{29}Si NMR and TGA. It was found that there was no Lewis acid–base interaction between PMMA and Al(OBu^s)(EAA)$_2$ complex. Octahedral aluminum was observed in the M5-Al(OBu^s)(EAA)$_2$ hybrids treated at temperature

below 200°C, and the trialkoxysilane-functional PMMA bonds with Al^{IV} and Al^{V} as PMMA was major in hybrid. The $T_{1\rho}^{H}$ value of the PMMA segments was consistent with that of the EAA segments indicated that they had the same mobility, and they were compatible in a nanometer scale estimated by spin-diffusion path length. However, the $T_{1\rho}^{H}$ values of M5-Al(OBu^{s})$(EAA)_2$-30 showed a larger value as compared with that of the other hybrids suggested that the motion of the EAA and PMMA segments in former was less restricted. The apparent activation energy E_a for random scission of EAA segments in hybrids was in the range of 58–34 kJ/mol, and that decreased roughly with increasing the PMMA content.

Acknowledgements

The authors thank the National Science Council of the Republic of China (Grant no. NSC 90-2113-M014-001). They would also like to thank Miss S.Y. Fang and Mr. Y.C. Lin for their expert technical assistance.

References

[1] M.M. Haridas, N. Goyal, J.R. Bellare, Ceram. Int. 24 (1998) 415.
[2] R. Nass, H.J. Schmidt, J. Non-Cryst. Solids 121 (1990) 329.
[3] C. Sanchez, L. Livage, M. Henry, F. Babonneau, J. Non-Cryst. Solids 100 (1988) 65.
[4] J.H. Wengrovius, M.F. Garbauskas, E.A. Williams, R.C. Going, P.E. Donahue, J.F. Smith, J. Am. Chem. Soc. 108 (1986) 982.
[5] T.C. Chang, Y.T. Wang, Y.S. Hong, Y.S. Chiu, J. Polym. Sci.: Part A: Polym. Chem. 38 (2000) 1972.
[6] T.C. Chang, Y.T. Wang, Y.S. Hong, H.B. Chen, J.C. Yang, Phosphorus, Sulfur and Silicon 160 (2000) 29.
[7] P.B. Maravalli, T.R. Goudar, Thermochim. Acta 325 (1999) 35.
[8] H.S. Bhojya Naik, Siddaramaiah, P.G. Ramappa, Thermochim. Acta 287 (1996) 279.
[9] K. Arora, Asian J. Chem. 7 (1995) 508.
[10] N.S. Bhave, V.S. Iyer, J. Therm. Anal. 32 (1987) 1369.
[11] N. Calu, L. Odochian, G.L. Brinzan, N. Bilba, J. Therm. Anal. 30 (1985) 547.
[12] D.W. van Krevelen, C. van Herden, F. Huntjens, J. Fuel 30 (1951) 253.
[13] S. Katyama, I. Yoshinaga, N. Yamada, Sol–Gel Optics IV Proc. SPIE 3136 (1997) 134.
[14] M.P.J. Peeters, A.P.M. Kentgens, Solid State Nucl. Magn. Reson. 9 (1997) 203.
[15] J. Livage, F. Babonneau, M. Chatry, L. Coury, Ceram. Int. 23 (1997) 13.
[16] T.C. Chang, Y.T. Wang, Y.S. Hong, C.T. Liu, Phosphorus, Sulfur and Silicon, 2001, in press.
[17] Y. Grohens, J. Schultz, R.E. Prud'homme, Int. J. Adhesion Adhesives 17 (1997) 163.
[18] M. Mehring, Principles of High Resolution NMR in Solids, 2nd Edition, Springer, Berlin, 1983, p. 260.
[19] P. Jackson, D. Carter, G. Dent, B.W. Cook, J.M. Chalmers, I.R. Dunkin, J. Chromatogr. A 685 (1994) 287.
[20] H.H.E. Kissinger, Anal. Chem. 29 (1957) 1702.